ARTICLE

Honokiol Nanoparticles in Thermosensitive Hydrogel: Therapeutic Effects on Malignant Pleural Effusion

Fang Fang,[†,#] ChangYang Gong,[†,⊥] ZhiYong Qian,[†,⊥,*] XiaoNing Zhang,[‡] MaLing Gou,[†] Chao You,[#] LiangXue Zhou,[†,#] JiaGang Liu,[#] Yu Zhang,[#] Gang Guo,[†] YingChun Gu,[†] Feng Luo,[†] LiJuan Chen,[†] Xia Zhao,[†] and YuQuan Wei[†]

[†]State Key Laboratory of Biotherapy and Cancer Center, West China Hospital, West China Medical School, Sichuan University, Chengdu, 610041, PR China, [#]Department of Neurosurgery, West China Hospital, Sichuan University, Chengdu, 610041, PR China, [‡]School of Medicine, Tsinghua University, Beijing, 100084, PR China, and [#]Department of Neurosurgery, West China Hospital, West China Medical School, Sichuan University, Chengdu, 610041, People's Republic of China. [⊥]C. Gong and Z. Qian contributed equally with F. Fang and are the cofirst authors for this paper.

ABSTRACT Honokiol (HK) can efficiently inhibit the growth of tumors. However, its clinical applications have been restricted by its extreme hydrophobicity. We hope to improve its water solubility by nanotechnology. And we wonder whether a novel honokiol nanoparticles-loaded thermosensitive poly(ethylene glycol)-poly(ε-caprolactone)-poly(ethylene glycol) (PEG-PCL-PEG, PECE) hydrogel (HK—hydrogel) could improve the therapeutic efficacy on malignant pleural effusion (MPE). To evaluate the therapeutic effects of HK—hydrogel on MPE, MPE-bearing mice were administered intrapleurally with HK—hydrogel, HK nanoparticles (HK—NP), blank hydrogel, or normal saline (NS) at days 4 and 11 after Lewis lung carcinoma (LLC) cells inoculation, respectively. Pleural tumor foci and survival time were observed, and antiangiogenesis of HK—hydrogel was determined by CD31. Histological analysis and assessment of apoptotic cells were also conducted in tumor tissues. HK—hydrogel reduced the number of pleural tumor foci, while prolonging the survival time of MPE-bearing mice, more effectively, as compared with control groups. In addition, HK—hydrogel successfully inhibited angiogenesis as assessed by CD31 ($P < 0.05$). Histological analysis of pleural tumors exhibited that HK—hydrogel led to the increased rate of apoptosis. This work is important for the further application of HK—hydrogel in the treatment of MPE.

KEYWORDS: honokiol · nanoparticles · biodegradable thermosensitive hydrogel · intrapleural administration · malignant pleural effusion

Honokiol (HK) is a bioactive compound extracted from *Magnolia officinalis* (Chinese name-,Houpo), which is used in traditional Chinese and Japanese medicine.[1,2] Extensive research has shown that honokiol can induce apoptosis, inhibit angiogenesis, and suppress the growth of tumor, representing a promising approach for malignancies treatment.[2−5] But administration of honokiol is greatly restrained due to its poor water-solubility. Nanotechnology provides an important method to overcome such shortcoming of hydrophobic drugs.[6−10] After processed into nanoparticles, such hydrophobic drugs could be well dispersed in water and form stable suspension to meet the requirement of administration.

Hydrogels are special materials which could absorb a considerable amount of water. For decades, thermosensitive hydrogels have attracted increasing attention owing to their biocompatibility and their remarkable response to environmental stimuli.[11−15] In this study, we prepared a kind of biodegradable and injectable poly(ethylene glycol)-poly(ε-caprolactone)-poly(ethylene glycol) (PEG-PCL-PEG, PECE) hydrogel controlled drug delivery system which undergoes sol−gel−sol transition with increase in temperature. The aqueous solution of PECE copolymers is free-flowing sol at ambient temperature and becomes gel at body temperature. This sol−gel transition behavior of PECE hydrogel gives the advantage of simply mixing it with pharmaceutical agents at room temperature in which it then becomes an *in situ* gel-forming controlled drug delivery system *in vivo* at body temperature about 37 °C.

Malignant pleural effusions (MPE) occur very frequently in patients with advanced cancer, predominantly adenocarcinoma of the lungs and other organs, and are associated with high morbidity and mortality. In addition, the presence of MPE severely compromised the patients' life quality.[16,17] Pleurodesis, indwelling pleural catheters and chemotherapy are commonly used to prevent symptomatic reaccumulation of pleural fluid; however, these therapies are nonspecific, often ineffective, and associated with morbidity.[18,19] Clearly, a more effective therapy for malignant pleural effusion is needed.

Herein, a novel drug delivery system was designed for achieving a sustained re-

*Address correspondence to anderson-qian@163.com.

Received for review July 11, 2009 and accepted November 8, 2009.

Published online November 18, 2009. 10.1021/nn900785b

lease of hydrophobic anticancer drug from the polymeric matrix. We then investigated the possible application of this drug delivery system for the treatment of experimental MPE by administrating the honokiol nanoparticles-loaded PECE hydrogel (HK−hydrogel) directly into the pleural cavity of MPE-bearing mice. Our experimental results demonstrated that such a strategy as this allows the carrier system to show a sustained release of honokiol *in vivo* as well as improved therapeutic effects on murine MPE.

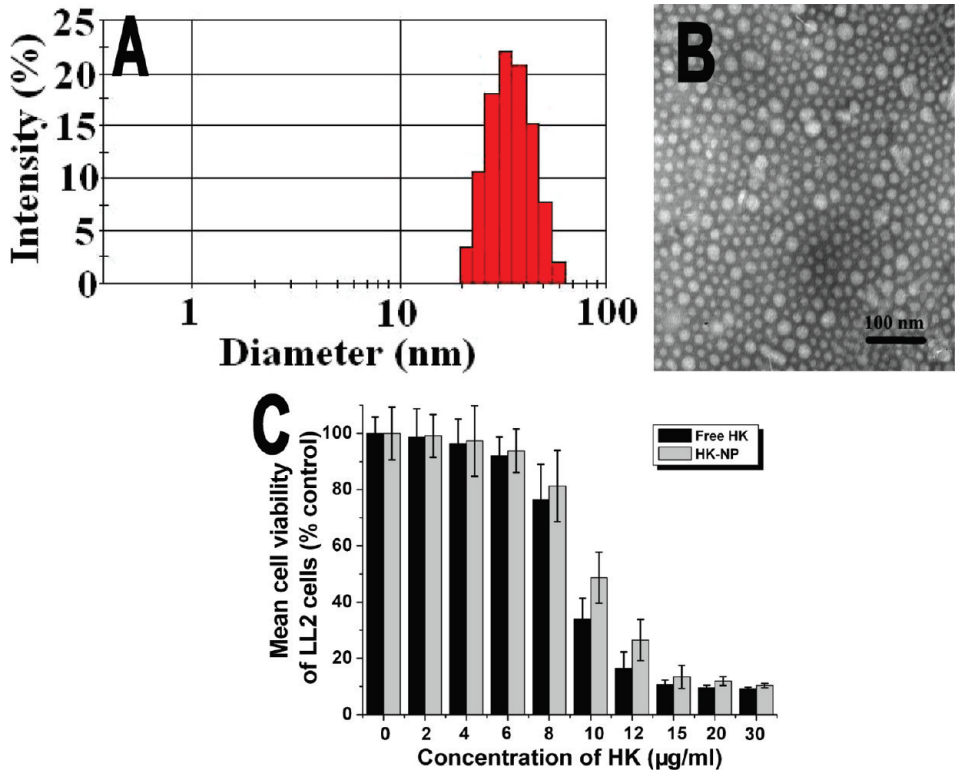

Figure 1. Preparation and characterization of HK−NP. (A) Particles size distribution spectrum of prepared HK−NP. The average particle size of prepared HK−NP was 33.34 ± 2.52 nm. (B) TEM image of prepared HK−NP. (C) *In vitro* tumor cell growth inhibition assay of LL2 cells. LL2 cells were exposed to different concentrations of free honokiol or HK−NP for 48 h, respectively. Error bars represent the standard deviation (n = 6).

RESULTS

Preparation and Characterization of HK−NP and HK-Hydrogel. Emulsion solvent evaporation method was used to prepare HK−NP. Figure 1A showed that the average particle size of HK−NP was 33.34 ± 2.52 nm, and polydisperse index (PDI) was 0.036. HK concentration of prepared HK−NP is 14.7 mg/mL, which is determined by HPLC. Figure 1B shows the TEM image of the HK−NP prepared. The TEM image revealed that HK−NP is monodispersed, thus confirming the spherical shape of HK−NP in solution. The MTT assay was performed to evaluate the toxicity of HK−NP and free honokiol to investigate whether nanoparticle influenced the cytotoxicity of honokiol. Both HK−NP and free honokiol at various concentrations significantly inhibited the growth of LL2 cells in a dose-dependent manner. Figure 1C presents the influence of drug concentration on cell viability of LL2 cells. The result indicates that the cytotoxicity of the HK−NP is comparable to that of free honokiol even though honokiol was released in an extended behavior.

The PECE copolymer was prepared by ring-opening copolymerization and coupling reaction. Chemical structure and molecular weight and distribution were characterized by ^{1}H NMR, FTIR, and GPC, which was reported in our previous article.[15] FTIR and ^{1}H NMR results indicated that the PECE triblock copolymer designed by controlling the feed composition were prepared successfully. The number-average molecular weight (M_n) and PEG/PCL ratio of PECE copolymer were calculated from ^{1}H NMR spectrum. M_n of PECE triblock copolymer was 3408 (480−2448−480). And the M_n and polydispersity (PDI) of PECE copolymer determined by GPC were 4391 and 1.30, respectively. As shown in Figure 2A, at low temperature, the hydrogel is an injectable flowing sol, and forms a non-flowing gel at body temperature.

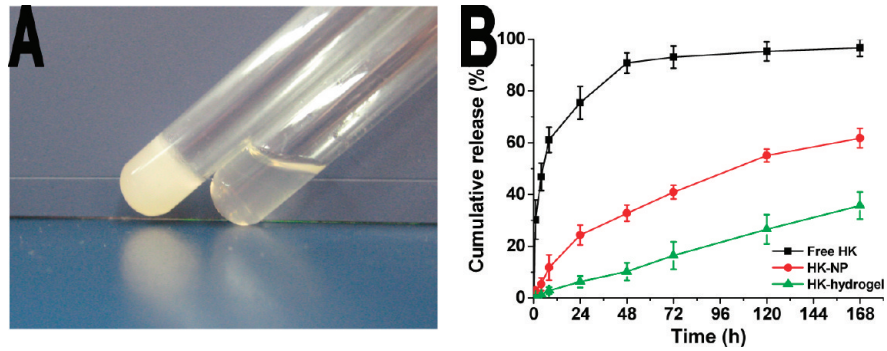

Figure 2. Preparation and characterization of HK−hydrogel (A) Photograph of HK−hydrogel at room temperature (right) and at 37 °C (left), respectively. At the concentration of 25 wt %, HK−hydrogel was free-flowing solution under 30 °C and became gel at body temperature to form *in situ* gel-forming controlled drug delivery system. (B) *In vitro* drug release profiles of free honokiol, HK−NP, and HK−hydrogel in PBS solution at pH 7.4. Error bars represent the standard deviation (n = 3).

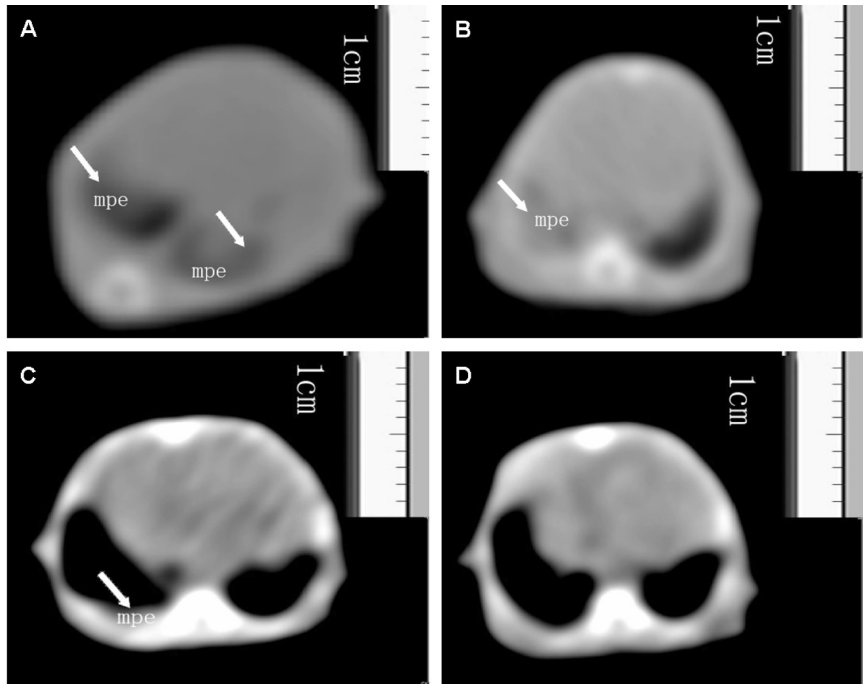

Figure 3. Representative CT imaging of malignant pleural effusions (transverse) After LLC cells inoculation, four groups of MPE-bearing mice were intrapleurally administered with 35 mg/kg HK−hydrogel at days 4 and 11, or honokiol, hydrogel, NS, respectively. At day 16 after LLC cells inoculation, transverse CT images of the three groups of mice showed that free-floating bilateral pleural effusions (mpe) were more clearly visible on CT scans in the mice of the two control groups administered with honokiol (C), hydrogel (B), or NS (A) as compared with that of the HK−hydrogel group (D).

Figure 2B presents the *in vitro* release profiles of free honokiol, HK−NP, and HK−hydrogel in PBS. In comparison with the release profile of free honokiol or HK−NP, the release rate of honokiol from hydrogel is much slower followed by a sustained release for up to 1 week. It was observed that only 10% of honokiol released from HK−hydrogel within 72 h, whereas free honokiol or HK−NP released approximately 91% or 33% into the outside media, respectively. This delay of drug release indicates their potential applicability in drug carrier to minimize the exposure of healthy tissues while increasing the accumulation of therapeutic drug in the tumor site.

Therapeutic Effects of HK-Hydrogel on MPE Formation and Pleural Tumors Dissemination. To determine the therapeutic effects of HK−hydrogel on MPE formation, C57BL/6 mice were inoculated with 2×10^5 LLC cells intrapleurally and treated with HK−hydrogel, HK−NP, hydrogel, or NS. To evaluate the presence of pleural effusions in the living animal, we performed CT on animals at day 16 after intrapleural tumor cells injection. The representative results were shown in Figure 3. Free-floating bilateral pleural effusions were clearly visible on CT scans of three control groups (Figure 3A,B,C). In contrast, malignant pleural effusions of the group administrated with HK−hydrogel were not very clearly visible on CT scans (Figure 3D).

At the time of harvest (18 days), pleural effusions of the three control groups could be directly visualized through the diaphragm, often surrounding tumor foci. The pleural tumors were found to reside equally on the visceral and parietal pleura (Figure 4A,B,C). However, the volume of pleural effusions and the number of pleural tumor foci decrease obviously with administration by HK−hydrogel (Figure 4D). Histology confirmed that pleural tumors consisted of adenocarcinomatous cells growing on the pleural surfaces (Figure 4E,F).

Features of MPE Generated in C57BL/6 Mice 18 Days after Intrapleural Administration. After mice were sacrificed by cervical dislocation and MPEs were harvested, we evaluated the characteristics of pleural fluid in four groups of C57BL/6 mice ($n = 10$ mice/group). The physical, cellular, and biochemical characters of the MPE obtained from mice of the four groups were presented (Figure 5). The pleural fluids of four groups all appeared hemorrhagic but did not coagulate, and after centrifugation the supernatants were straw colored, but the colors of the MPE in the three control groups were clearly deeper than that of the HK−hydrogel group (data not shown). As shown in Figure 5A, the mean MPE volume was clearly reduced in the HK−hydrogel group (204.6 ± 27.3 μL) as compared with that in the HK−NP (507 ± 58.2 μL, $P < 0.05$), hydrogel (629.7 ± 62.5 μL, $P < 0.05$) or NS group (603.4 ± 49.5 μL, $P < 0.05$). As compared with the HK−NP (pleural tumor foci, 7.43 ± 0.79, $P < 0.05$; tumor cells in MPE, 9.17 ± 0.59, × 10^3/μL, $P < 0.05$), hydrogel (pleural tumor foci, 11.28 ± 3.1, $P < 0.05$; tumor cells in MPE, 15.87 ± 0.56, × 10^3/μL, $P < 0.05$), or NS group (pleural tumor foci, 11.58 ± 2.72, $P < 0.05$; tumor cells in MPE, 16.21 ± 0.87, × 10^3/μL, $P < 0.05$), the significant reductions in the number of pleural tumor foci and tumor cells of MPE were observed in the HK−hydrogel group (pleural tumor foci, 4.02 ± 0.64; tumor cells in MPE, 5.23 ± 0.48, × 10^3/μL) (Figure 5B). Obviously, the number of red blood cells of MPE in the HK−hydrogel group (3.87 ± 0.51, × 10^3/μL) was lower than that in the HK−NP (4.63 ± 0.25, × 10^3/μL, $P < 0.05$), Hydrogel (5.69 ± 0.37, × 10^3/μL, $P < 0.05$) or NS group (5.28 ± 0.32, × 10^3/μL, $P < 0.05$) (Figure 5C). Biochemical assay indicated that the levels of total protein and LDH in MPE of the Honokiol (total protein, 36.48 ± 2.57 g/L, $P < 0.05$; LDH, 4521 ± 237 IU/L, $P < 0.05$), hydrogel (total protein, 39.40 ± 3.02 g/L, $P < 0.05$; LDH 6263 ± 410 IU/L, $P < 0.05$) or NS group (total protein, 42.93 ± 2.43 g/L, $P < 0.05$; LDH 6634 ± 426 IU/L, $P < 0.05$) were sig-

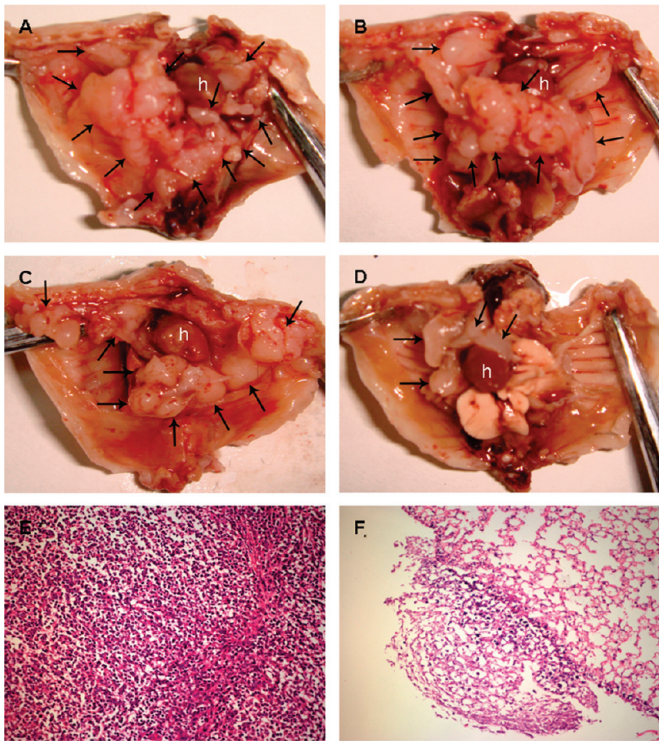

Figure 4. Representative malignant pleural tumors in C57B/6 mice after intrapleural administration. At day 7 after the completion of treatment as described in the Experimental Details, mice (n = 10 mice/group) were sacrificed by cervical dislocation, MPEs were gently aspirated, and chest walls were opened. Lung and chest wall explants showed multiple tumor foci (arrows) on the parietal and visceral pleura. Significantly decreased number of pleural tumor in HK−hydrogel treated group (D) as compared with the NS (A), hydrogel (B), or honokiol (c) groups were shown (h: heart). Section (×200) through a small visceral pleural Lewis lung cancer implantation stained with hematoxylin and eosin shows that pleural tumors consisted of adenocarcinomatous cells (E), and tumors grew on the pleural surface (F).

nificantly higher than those in the HK−hydrogel group (total protein, 32.53 ± 2.77 g/L; LDH, 3047 ± 198 IU/L) (Figure 5D,E). In addition, VEGF protein level in MPE of the HK−hydrogel group (515.7 ± 38.2 pg/mL) was decreased about 4-fold below that in the pleural fluids from the HK−NP (1731 ± 45.3 pg/mL, $P < 0.05$), hydrogel(2216.6 ± 94.5 pg/mL, $P < 0.05$) or NS groups (2270 ± 124 pg/mL, $P < 0.05$) (Figure 5F).

To determine whether intrapleural administration with HK−hydrogel in this MPE model could decrease vascular permeability, we measured leakage of Evans' blue dye into the pleural space. The results indicated that the absorbance values at a wavelength of 630 nm of HK−hydrogel group (A_{630nm}, 0.053 ± 0.004; $P < 0.05$) was obviously lower than that in the HK−NP (A_{630nm}, 0.163 ± 0.016; $P < 0.05$), hydrogel (A_{630nm}, 0.30 ± 0.03; $P < 0.05$), or NS group (A_{630nm}, 0.33 ± 0.04; $P < 0.05$) (Figure 5G).

Treatment with HK−Hydrogel Inhibited Tumor Vascularization. To better understand the mechanism by which treatment with HK−hydrogel inhibited MPE formation, the microvessel density of four groups was measured. Pleural tumors distributed between visceral and parietal pleural surface were harvested, fixed in formalin, and paraffin-embedded sections were stained with anti-CD31 antibody. Immunohistochemistry demonstrated reduction of microvessel density in HK−hydrogel group relative to the three control groups (Figure 6).

Therapeutic Effects on Apoptosis. To explore the role of HK−hydrogel on apoptosis of pleural tumor cells, tumor resections were subjected to terminal dUTP nick end labeling (TUNEL) assays for respective determination of apoptotic index. HK−NP treatment affected the apoptosis rate of tumor cells (Figure 7B), whereas the density of apoptotic cancer cells increased after administration of HK−hydrogel (Figure 7A). Data represent the mean apoptotic index ± standard deviations of cancer cells as percent normalized to apoptotic index of cancer cells (Figure 7E).

Treatment with HK−hydrogel Improved Survival Time. Life span analysis (Figure 8) showed that control animals that received the hydrogel and NS treatment survived 18 and 16.5 days on average, while HK−NP group survived 24.9 days on average. In contrast, treatment with HK−hydrogel resulted in a significant increase in life span ($P < 0.01$, Figure 6), and 50% of the animals still survived at day 35 after treatment.

DISCUSSION

Malignant pleural effusion is a very common, difficult to treat, and debilitating occurrence in patients with cancer. Strategies such as sustained and localized therapy may have the potential to improve the efficacy of medical treatment.[20] The present study explored the feasibility of using novel nanoparticles-loaded thermosensitive hydrogel based on biodegradable PECE copolymer for controlled release of honokiol, and the therapeutic effects of this drug delivery system for the treatment of experimentally-induced MPE. Our results showed that intrapleural administration of HK−hydrogel would efficiently increase tumor cell apoptosis, decrease pleural vascular permeability, and reduce new blood vessel formation in pleural tumors.

HK is a multifunctional drug which can induce apoptosis, suppress tumor growth, and inhibit angiogenesis, and it has great potential in disease therapy especially in cancer therapy.[21−23] A rapid separation approach had been developed using high-capacity high-speed counter-current chromatography (high-capacity HSCCC) to isolate and purify honokiol from Houpu by Chen *et al.* in our laboratory.[24] However, its

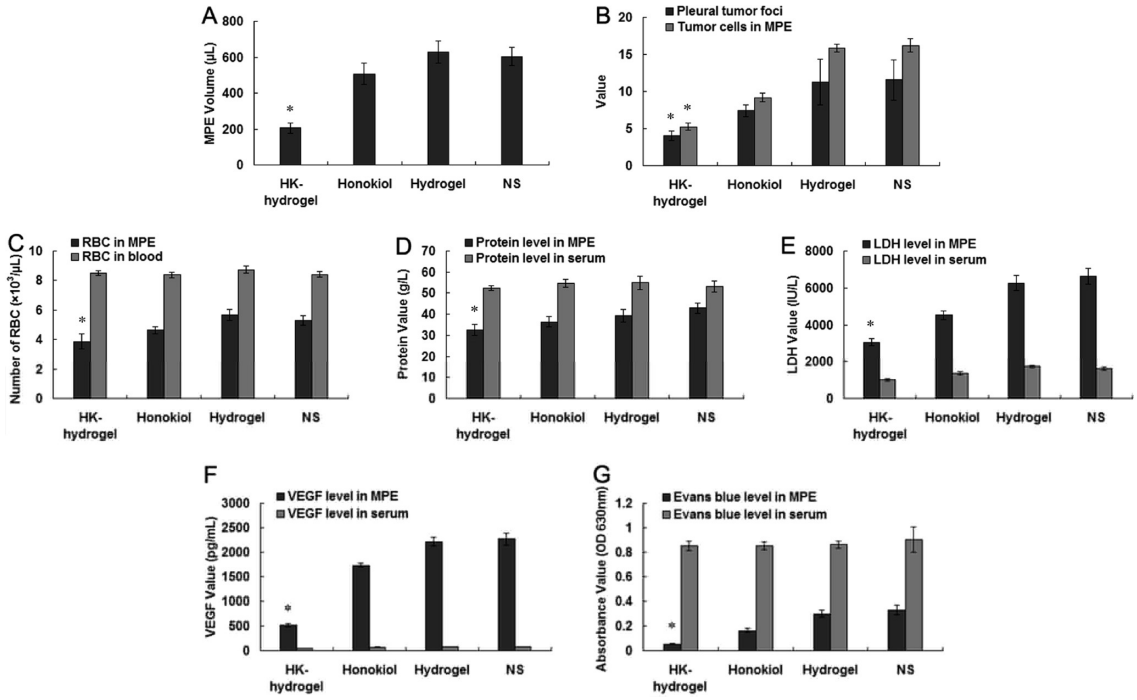

Figure 5. Features of MPE generated in C57BL/6 mice 18 days after intrapleural administration. At day 7 after the completion of treatment, mice (n = 10 mice/group) were sacrificed by cervical dislocation and blood was drawn from the retro-orbital veins. Then, the abdominal walls of mice were cut down, the diaphragms were exposed, and MPEs were gently aspirated using a 1-ml syringe. The volume of MPE was measured with the syringe. The mean MPE volume was clearly reduced in the HK−hydrogel group as compared with the control groups (A). Tumor implantations on the pleura were counted by two independent readers under a dissecting microscope, and the average number was used for data analyses. The number of pleural tumor foci and tumor cells in MPE of the HK−hydrogel group were significantly reduced as compared with the control groups (B). The number of red blood cells in MPE of the HK−hydrogel group was lower than that in the three control groups (C). Serum and pleural fluid samples were assayed for total protein content, LDH, and VEGF. The levels of total proteins (D) and LDH (E) in MPE of the three control groups were significantly higher than those in the HK−hydrogel group. In addition, VEGF protein level (F) in MPE of the HK−hydrogel group was significantly reduced about 4-fold as compared with the honokiol group. To evaluate the pleural permeability of the mice, at day 7 after the completion of treatment, each mouse (n = 8 mice/group) received 200 μL of 5 mg/mL Evans' blue solution (total dose 1 mg) intravenously and was sacrificed 2 h later. Pleural fluid and serum Evans' blue concentration were determined by measuring absorbance at a wavelength of 630 nm in a spectrophotometer. The absorbance value in the MPE of the HK−hydrogel group was obviously lower than that in the three control groups (G): (columns) mean value of each group; (bars) ±SD; (*) $P < 0.05$ compared with NS, hydrogel or honokiol group.

further application was restrained due to its great hydrophobicity. To overcome such a shortcoming of honokiol crystal, we prepared novel HK−NP.[10] The obtained HK−NP could be well-dispersed in water, and it is stable. The maximum concentration of HK−NP was up to 25 mg/mL. The average particle size of prepared HK−NP was 33.34 nm and the nanoparticles have a small negative zeta potential (about −0.385 mv) close to neutral.

Over past decades, *in situ* gel-forming controlled drug delivery system has received considerable attention owing to the simplicity of pharmaceutical formulation by solution mixing and the sustained ability of drug delivery.[25−28] The *in situ* gel-forming controlled drug delivery system enables drugs to be easily mixed and to form a depot by syringe injection at a target location, in which the depot works as a sustained drug delivery system. In particular, the thermosensitive physical hydrogel based on synthetic block copolymers has been extensively studied since its potential biomedical applications in the *in situ* gel-forming controlled drug delivery system.[29−32] PCL and PEG are both well-known FDA-approved biodegradable and biocompatible materials, which have been widely used in the biomedical field. Due to the combination of great advantages of PEG and PCL, the PECE hydrogels have great potential application as an *in situ* gel-forming controlled drug delivery system. According to our previous work, no LD50 of the PECE hydrogel system could be determined due to the great biocompatibility of PEG and PCL.[33] The maximal tolerance dose (MTD) of the PECE hydrogel system is higher than 10 g/kg body weight, which is much higher than the dose used as a drug carrier. The results indicate that PECE hydrogel might be a safe candidate for *in situ* gel-forming controlled drug delivery system.

In the present studies, biodegradable PECE hydrogel was synthesized which undergoes a special thermosensitive sol−gel−sol transition. The hydrogel is a free-flowing sol at room temperature or below critical gelation temperature (CGT), becomes gel at body temperature, and could sustain long time periods for *in situ*

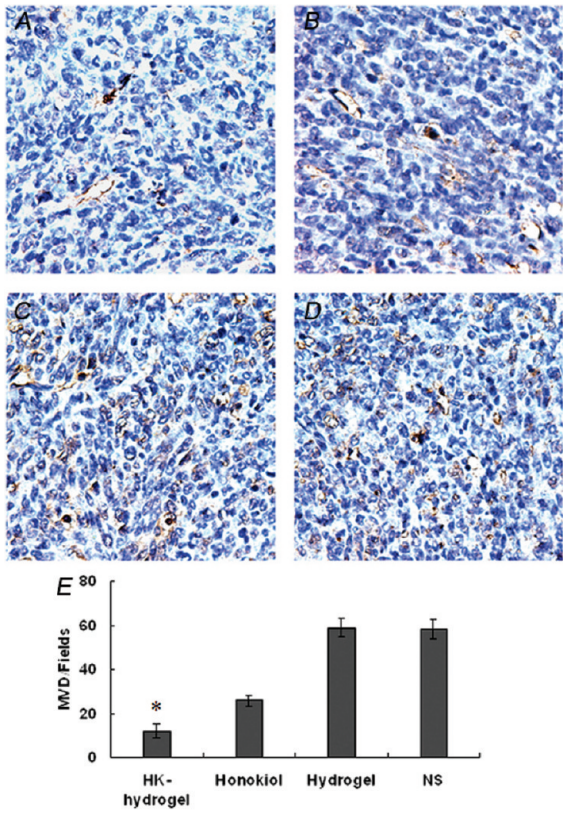

Figure 6. Inhibition of tumor vascularization by immunohistochemistry with CD31. Pleural tumor angiogenesis was assessed by immunohistochemical staining with anti-CD31 antibody (brown) on paraffin-embedded sections of tumors resected 7 days after the completion of treatment. Microvessel counting was done at ×200. Tumors of the HK−hydrogel group revealed only occasional, isolated microvessels (A). At the same magnification, the section of representative images with well-formed capillaries surrounding nests of tumor cells in hydrogel (C) or NS (D) control treated group. HK−hydrogel treatment group displayed decreased microvessel as compared with the three control groups in pleural tumor tissues (E). (Columns) mean of microvessel per high-power field; (bars) ±SD; (*) $P < 0.05$ compared with honokiol, hydrogel, or NS group.

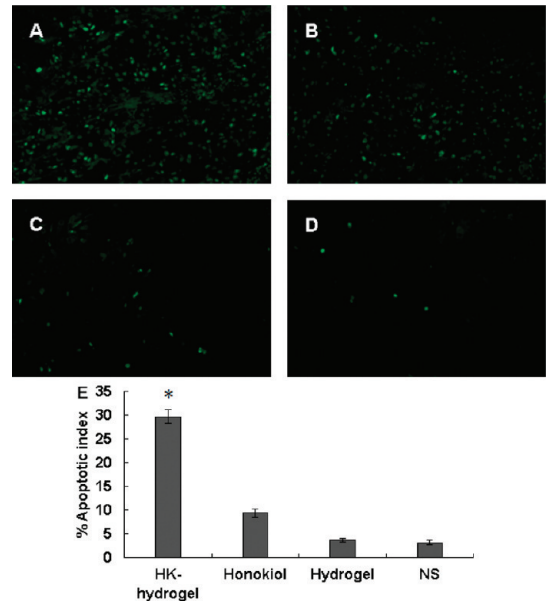

Figure 7. TUNEL staining of pleural tumor tissues. Pleural tumor tissues preparation and procedure for TUNEL staining were described in Experimental Details. Representative sections from pleural tumor tissue are presented: HK−hydrogel (A), honokiol (B), hydrogel (C), or NS (D). Bar represented apoptotic index within tissue from LL2 from 10 mice (E). (*) $P < 0.05$ compared with honokiol, hydrogel, or NS group.

drug release (Figure 1C). Honokiol nanoparticles-loaded hydrogel composite system could release the drug in an extended period at effective level *in vivo*. In addition, the drug delivery system could reduce the burst release ratio of honokiol, which means that the complex can reduce the toxic side-effects of honokiol and elevate tolerance and drug availability.

In the preliminary experiment, we performed a dose gradient assay *in vivo*. Mice were divided into four groups ($n = 5$) treated with hydrogel- loaded different doses of HK (10, 20, 35, and 50 mg/kg). However, two mice of the 50 mg/kg HK group died in the second day after administration. Of the other three groups, the 35 mg/kg group had the best therapeutic effects. When the HK dose was too high, the side-toxic effect was enhanced; when the HK dose was low, the anticancer effect was too low. As a result, the dose of HK at 35 mg/kg was selected for further study in this work.

The present studies demonstrated that therapy with HK−NP resulted in reduced pleural tumor foci, whereas sustained honokiol treatment by intrapleural administration of HK−hydrogel had the more efficiently therapeutic effects and significantly improved the survival rate(Figure 8). Compared with the nontreated control (NS group), the MPE volume was reduced by 16% in the HK−NP treated group after the completion of treatment and was reduced by 66.1% in the HK−hydrogel treated group (Figure 5). Furthermore, control animals that received NS and hydrogel treatment survived 16.5 and 18 days on average, respectively. In contrast, HK−hydrogel treatment resulted in about 2-fold increase in life span.

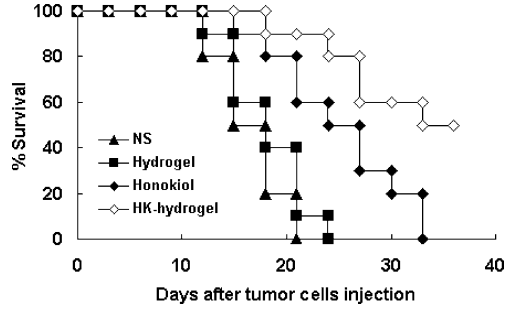

Figure 8. Survival advantage in Mice. Mice (10 mice per group) were administered intrapleurally with the HK−hydrogel at 35 mg/kg HK−hydrogel at days 4 and 11, or honokiol, hydrogel, or NS, respectively. Life span analysis showed that neither hydrogel group nor NS group survived 18 and 16.5 days on average. A significant increase in survival in the HK−hydrogel group compared with the three control groups ($P < 0.01$, by log-rank test) was found in this mouse model.

Although the mechanism by which HK−hydrogel can inhibit the formation and progression of MPE remained to be determined completely, the anti-MPE efficacy *in vivo* may in part result from sustained delivery of honokiol, which may inhibit tumor cell proliferation and limit the emergence of malignant cell populations, more efficiently block the formation of new blood vessels, and increase induction of the apoptosis in the pleural tumors. This suggestion is supported by the present findings. HK−hydrogel did remarkably decrease microvessel density in pleural tumors compared to the other three control groups (Figure 5). Previous studies indicated that honokiol could down-regulate the expression of vascular endothelial growth factor (VEGF),[34] which has been shown to play an important role in the formation of exudative PEs, and VEGF blockage will significantly reduce vascular permeability and pleural fluid (PF) accumulation in a murine model of MPE.[35−38] Our findings that decreasing microvessel density and VEGF protein levels by administration with HK−hydrogel coincide with previous reports. In addition, the more-apparent apoptotic cells in the tumors treated with HK−hydrogel were found, compared with the treatment with HK−NP alone or no-treatment groups.[2,34,37−40]

CONCLUSIONS

In this paper, we successfully prepared a novel honokiol nanoparticles loaded thermosensitive hydrogel based on biodegradable PECE copolymer (HK−hydrogel). And the therapeutic effects of HK−hydrogel in C57BL/6 mice model of MPE by intrapleural administration directly were investigated. Our results showed that HK−NP could be dispersed in water very easily, and the HK−hydrogel system can enhance the therapeutic effects and diminish the side effects of honokiol. According to our experiment, we found that intrapleural administration of HK−hydrogel could significantly inhibit the formation and progression of malignant pleural effusion. Given the uniformly poor prognosis of patients with MPE, the findings provide an ideal scenario by which the future clinical trials can be contemplated.

EXPERIMENTAL DETAILS

Materials. ε-Caprolactone (ε-CL, Alfa Aesar, USA), poly(ethylene glycol) methyl ether (MPEG, M_W = 550, Aldrich, USA), stannous octoate ($Sn(Oct)_2$, Sigma, USA), hexamethylene diisocyanate (HMDI, Aldrich, USA), pluronic F127 (Sigma, USA), and ethyl acetate (Et Ac, KeLong Chemicals, China) were used without any further purification. All the materials used in this article were analytic reagent (AR) grade and used as received. Honokiol was purified in our lab by L. J. Chen *et al.* using high-speed countercurrent chromatography, and the purity is above 99.5%.[24]

Preparation of Honokiol Nanoparticles (HK−NP). A 60 mg portion of HK was dissolved in 2 mL of EtAc to form HK solution. Then, the HK−EtAc solution was introduced into 4 mL of F127 aqueous solution (5%w/w) under stirring at approximately 15000 rpm by T10 homogenizer (IKA, German). About 10 min later, the O/W emulsion was formed. Then, the EtAc was evaporated in rotator evaporator (BÜCHI, Switzerland) and HK−NP were obtained. The HK−NP slurry was lyophilized, and the obtained powder was stored at 4 °C before further use. Detection of particle size and zeta potential, morphology study, and cytotoxicity assay of HK−NP were conducted.[10]

Synthesis and Characterization of PECE Hydrogel. PEG-PCL diblock copolymer was prepared by ring-opening copolymerization of ε-CL initiated by MPEG using stannous octoate as catalyst; PEG−PCL−PEG triblock copolymer was synthesized by coupling PEG−PCL diblock copolymer using HMDI as coupling agent, which has been reported previously.[15] The phase transition of PECE hydrogel was recorded using test tube-inverting method. Conditions of gel and sol were defined as "no flow" and "flow" in 1 min, respectively, when the test tube was inverted. Each sample at the given concentration was prepared by dissolution in deionized water at the designated temperature. The volume of the solution was kept 1 mL in total regardless of the concentration. The hydrous samples were incubated in a water bath at 0 °C for 20 min, and then slowly heated at a heating rate of 0.5 °C/min, from 0 °C to the temperature when precipitation occurred.

Preparation of Honokiol Nanoparticles-Loaded Hydrogel (HK−Hydrogel). PECE copolymer was dissolved in normal saline (NS) at the designated temperature, and then the solution was kept at 0 °C. After that, HK−NPs were added into the hydrogel solution to form a homogeneous HK−hydrogel complex, and the concentration of the hydrogel complex was adjusted to 25 wt % containing a designed amount of honokiol.

***In Vitro* Drug Release Behavior of Honokiol.** *In vitro* release behavior of honokiol from nanoparticles or hydrogels was determined by a modified dialysis method as follows: 500 μL of HK−NP solution or HK−hydrogel solution (25 wt %) was placed in a dialysis tube (molecular weight cutoff (MWCO) is 3.5 kDa, and the dialysis area is 1 cm^2), and 0.5 mL of honokiol solution in DMSO was used as control. The concentration of HK in HK−hydrogel, HK−NP, or HK−DMSO was kept at 1 mg/mL, respectively. The dialysis tubes were incubated in 10 mL of PBS (prewarmed to 37 °C, pH = 7.4) containing Tween80 (0.5 wt %) at 37 °C with gentle shaking (100 rpm), and the release media were displaced by prewarmed fresh PBS at a predetermined time. The supernatant of the removed release media were collected and stored at −20 °C before further analysis. The released drug was quantified using high-performance liquid chromatography (HPLC). All results were the mean of three test runs, and all data were expressed as the mean ±SD.

Cell Culture, Animal Model, and Treatment Plan. The LLC cells were purchased from the American Type Culture Collection (Manassas, VA) and were cultured at 37 °C in 5% CO_2−95% air using Dulbecco's modified Eagle's medium (DMEM) with 10% fetal bovine serum. Female (6−8 weeks old) C57BL/6 mice (purchased from the Laboratory Animal Center of Sichuan University) were acclimatized for 1 week. All animal care and experimental procedures were approved by and conducted according to Institutional Animal Care and Use guidelines.

For establishment of the MPE model, mice were anesthetized using pentobarbital sodium prior to all procedures. LLC cells (2×10^5) suspended in 50 μL of PBS were injected into the pleural cavity through the intercostal space directly. The animals were observed until complete recovery. The procedure was not associated with mortality or morbidity.

After LLC cells inoculation, mice were randomly divided into four groups (n = 28 mice/group): (1) HK−hydrogel group, each animal was intrapleurally injected with 35 mg/kg of HK−hydrogel (150 μL) at day 4 and 11 (once a week, twice totally); (2) HK−NP group, each animal was intrapleurally injected with 35 mg/kg of HK−NP suspended in normal saline (150 μL) at day 4 and 11 (once a week, twice totally); (3) hydrogel group, each animal was intrapleurally injected with equal volume of PECE hydrogel at day 4 and 11 (once a week, twice totally); and

(4) NS group, each animal was intrapleurally injected equal volume of NS on the same schedule as mentioned above. The effective dose was chosen according to preliminary experiment.

For MPE growth study ($n = 10$ mice/group), at day 5 after the final administration (day 16 after LLC cells inoculation), computed tomography (CT) images were acquired for all the mice in all four groups, and then at day 18 after LLC cells inoculation, mice were sacrificed by cervical dislocation and blood was drawn from the retro-orbital veins. Then, the abdominal walls of the mice were cut down, and the viscera were retracted to visualize the diaphragm. Pleural fluid was gently aspirated using a 1-ml syringe, and its volume was measured by the syringe. For histopathological study, tumors, lungs, chest walls, and major organs were inflated, explanted, and fixed with 10% neutral buffered formalin.

The experiment for observation of survival advantage included 10 mice per group, and mice without heartbeat and breathing were determined to be dead. The other 8 mice per group were used for pleural permeability assay.

Therapeutic Effects Evaluation of Model Animal Experiments. CT images were acquired on a Siemens Somatom Sensation16 using a tube voltage of 120 kVp and current of 93 μA. Mice were under anesthesia as described previously during imaging session. The animal holder possessed four fiducial markers visible in CT, which facilitated coregistration of the images using the SIENET Sky-VA50B DICOM-CD Viewer (Siemens AG, Erlangen, Germany).

Because pleural tumors were evenly distributed between visceral and parietal pleural surfaces, only visceral implantations were enumerated, excluding primary tumors at the injection site that occurred occasionally. Pleural tumors were counted by two independent and blinded readers under a dissecting microscope, and the average number was used for data analysis. Mice lungs, chest walls, and major organs were fixed in 10% neutrally buffered formalin for 24 h and 70% ethanol for 3 days. Tissues were embedded in paraffin, and 5-μm-thick sections were cut, mounted on glass slides, and stained with hematoxylin-eosin (H&E). Pleural fluid and serum levels of glucose, total protein content, and lactate dehydrogenase (LDH) were determined enzymatically on the Olympus AU400 Clinical Clinic Chemistry analyzer (Olympus Diagnostic, Japan). Serum and pleural fluid samples were assayed for vascular endothelial growth factor (VEGF) using commercially available mouse ELISA kits (R&D Systems, Minneapolis, MN) according to the manufacturer's instructions.

Pleural Permeability Assay and Detection of Microvessel Density. Mice of HK−hydrogel group ($n = 8$ mice/group, 18 ays 18 after LLC inoculation) and the other three groups respectively received 200 μL of Evans' blue solution (5 mg/mL, total dose 1 mg) intravenously and were sacrificed 2 h later. Evans blue concentration of pleural fluid and serum were determined by measuring absorbance at 630 nm in a spectrophotometer.

Blood vessels in pleural tumors growing on the visceral and parietal pleural surfaces of C57BL/6 mice were counted under light microscope after immune staining of sections with polyclonal goat antimouse CD31 antibody (1:200; Santa Cruz Biotechnol Inc., Santa Cruz, CA) at 4 °C overnight, followed by incubation with biotinylated polyclonal rabbit antigoat antibody (1:200; Vector Laboratories, Inc., Burlingame, CA). Positive reaction was visualized using 3,3-diamino-benzidine as chromagen (DAB substrate kit; Vector). Sections were counterstained with hematoxylin and mounted with glass coverslips. Then sections were visualized in an Olympus microscope. The results regarding angiogenesis were expressed as the absolute number of the microvessel per high-power field of three sections in each pleural tumor, as described previously.[41,42]

Quantitative Assessment of Apoptosis. At day 18 after LLC cells inoculation, pleural tumor species were prepared as described above. TUNEL staining was performed using an *in situ* cell death detection kit (Roche Molecular Biochemicals) following the manufacturer's protocol, as previously described.[41,42]

It is based on the enzymatic addition of digoxigenin−nucleotide to the nicked DNA by terminal deoxynucleotidyl transferase. In tissue sections four equal-sized fields were randomly chosen and analyzed. Density was evaluated in each field, yielding the density of apoptotic cells (apoptosis index).

Statistics Analysis. Experiments were done at least in triplicate. The statistic analysis was carried out using SPSS 13 (Chicago, IL, USA). Data was assayed by ANOVA and Student's *t* test. For the survival time of animals, Kaplan−Meier curves were established for each group, and the survivals were compared by the means of log-rank test. Differences between means or ranks, as appropriate, were considered significant when yielding a $P < 0.05$.

Acknowledgment. This work was financially supported by National 863 project (2007AA021902 and 2007AA021804), National Natural Science Foundation of China (NSFC20704027), Specialized Research Fund for the Doctoral Program of Higher Education (200806100065), New Century Excellent Talents in University (NCET-08-0371), and Chinese Key Basic Research Program (2010CB529906). We have no conflict of interest for this work.

REFERENCES AND NOTES

1. Watanabe, K.; Watanabe, H.; Goto, Y.; Yamaguchi, M.; Yamamoto, N.; Hagino, K. Pharmacological Properties of Magnolol and Honokiol Extracted from Magnolia Officinalis: Central Depressant Effects. *Planta Med.* **1983**, *49*, 103–108.
2. Ishitsuka, K.; Hideshima, T.; Hamasaki, M.; Raje, N.; Kumar, S.; Hideshima, H.; Shiraishi, N.; Yasui, H.; Roccaro, A. M.; Richardson, P.; *et al*. Honokiol Overcomes Conventional Drug Resistance in Human Multiple Myeloma by Induction of Caspase-Dependent and -Independent Apoptosis. *Blood.* **2005**, *106*, 1794–1800.
3. Bai, X.; Cerimele, F.; Ushio-Fukai, M.; Waqas, M.; Campbell, P. M.; Govindarajan, B.; Der, C. J.; Battle, T.; Frank, D. A.; Ye, K.; *et al*. Honokiol, a Small Molecular Weight Natural Product, Inhibits Angiogenesis *in Vitro* and Tumor Ggrowth *in Vivo*. *J. Biol. Chem.* **2003**, *278*, 35501–35507.
4. Wolf, I.; O'Kelly, J.; Wakimoto, N.; Nguyen, A.; Amblard, F.; Karlan, B. Y.; Arbiser, J. L.; Koeffler, H. P. Honokiol, a Natural Biphenyl, Inhibits *in Vitro* and *in Vivo* Growth of Breast Cancer Through Induction of Apoptosis and Cell Cycle Arrest. *Int. J. Oncol.* **2007**, *30*, 1529–1537.
5. Shigemura, K.; Arbiser, J. L.; Sun, S. Y.; Zayzafoon, M.; Johnstone, P. A.; Fujisawa, M.; Gotoh, A.; Weksler, B.; Zhau, H. E.; Chung, L. W. Honokiol, a Natural Plant Product, Inhibits the Bone Metastatic Growth of Human Prostate Cancer Cells. *Cancer.* **2007**, *109*, 1279–1289.
6. Chawla, J. S.; Amiji, M. M. Biodegradable Poly(epsilon-caprolactone) Nanoparticles for Tumor-Targeted Delivery of Tamoxifen. *Int. J. Pharm.* **2002**, *249*, 127–138.
7. Allen, T. M.; Cullis, P. R. Drug Delivery Systems: Entering the Mainstream. *Science.* **2004**, *303*, 1818–1822.
8. Farokhzad, O. C.; Cheng, J.; Teply, B. A.; Sherifi, I.; Jon, S.; Kantoff, P. W.; Richie, J. P.; Lang, R. Targeted Nanoparticle-Atapmer Bioconjugates for Cancer Chemotherapy *in Vivo*. *Proc. Natl. Acad. Sci. U.S.A.* **2006**, *103*, 6315–6320.
9. Kesisoglou, F.; Panmai, S.; Wu, Y. Nanosizing—Ooral Formulation Development and Biopharmaceutical Evaluation. *Adv. Drug Delivery Rev.* **2007**, *59*, 631–644.
10. Gou, M. L.; Dai, M.; Li, X. Y.; Wang, X. H.; Gong, C. Y.; Xie, Y.; Wang, K.; Zhao, X. Z.; Qian, Y.; Wei, Y. Q. Preparation and Characterization of Honokiol Nanoparticles. *J. Mater. Sci., Mater. Med.* **2008**, *19*, 2605–2608.
11. Jeong, B.; Bae, Y. H.; Lee, D. S.; Kim, S. W. Biodegradable Block Copolymers as Injectable Drug-Delivery Systems. *Nature* **1997**, *388*, 860–862.
12. Kissel, T.; Li, Y.; Unger, F. ABA-Triblock Copolymers from Biodegradable Polyester A-Blocks and Hydrophilic Poly(ethylene oxide) B-Blocks as a Candidate for *in Situ* Gorming Hydrogel Delivery Systems for Proteins. *Adv. Drug Delivery Rev.* **2002**, *54*, 99–134.
13. Jeong, B.; Kim, S. W.; Bae, Y. H. Thermosensitive Sol−Gel Reversible Hydrogels. *Adv. Drug Delivery Rev.* **2002**, *54*, 37–51.
14. Ruel-Gariépy, E.; Leroux, J. C. *In Situ*-Forming Hydrogels—Review of Temperature-Sensitive Systems. *Eur. J. Pharm. Biopharm.* **2004**, *58*, 409–426.

15. Gong, C. Y.; Shi, S.; Dong, P. W.; Kan, B.; Gou, M. L.; Wang, X. H.; Li, X. Y.; Luo, F.; Zhao, X.; Wei, Y. Q.; Qian, Z. Y. Synthesis and Characterization of PEG−PCL−PEG Thermosensitive Hydrogel. *Int. J. Pharm.* **2009**, *365*, 89–99.
16. Antony, V. B.; Loddenkemper, R.; Astoul, P.; Boutin, C.; Goldstraw, P.; Hott, J.; Panadero, F. R.; Sahn, S. Management of Malignant Pleural Effusions. *Am. J. Respir. Crit. Care Med.* **2000**, *162*, 1987–2001.
17. Burrows, C. M.; Mathews, W. C.; Colt, H. G. Predicting Survival in Patients with Recurrent Symptomatic Malignant Pleural Effusions. *Chest* **2000**, *117*, 73–78.
18. Light, R. W. Talc for Pleurodesis? *Chest* **2002**, *122*, 1506–1508.
19. Maskell, N. A.; Lee, Y. C.; Gleeson, F. V.; Hedley, E. L.; Pengelly, G.; Davies, R. J. Randomized Trials Describing Lung Inflammation after Pleurodesis with Talc of Varying Particle Size. *Am. J. Respir. Crit. Care Med.* **2004**, *170*, 377–382.
20. Vassileva, V.; Allen, C. J.; Piquette-Miller, M. Effects of Sustained and Intermittent Paclitaxel Therapy on Tumor Repopulation in Ovarian Cancer. *Mol. Cancer Ther.* **2008**, *7*, 630–637.
21. Maruyama, Y.; Kuribara, H. Overview of the Pharmacological Features of Honokiol. *CNS Drug Rev.* **2000**, *6*, 35–44.
22. Battle, T. E.; Arbiser, J.; Frank, D. A. The Natural Product Honokiol Induces Caspase-Dependent Apoptosis in B-Cell Chronic Lymphocytic Leukemia (B-CLL) Cells. *Blood* **2005**, *106*, 690–697.
23. Li, L.; Han, W.; Gu, Y.; Qiu, S.; Lu, Q.; Jin, J.; Luo, J. H.; Hu, X. Honokiol Induces a Necrotic Cell Death through the Mitochondrial Permeability Transition Pore. *Cancer Res.* **2007**, *67*, 4894–4903.
24. Chen, L. J.; Zhang, Q.; Yang, G. L.; Fan, L. Y.; Tang, J.; Garrard, I.; Ignatova, S.; Fisher, D.; Sutherland, I. A. Rapid Purification and Scale-up of Honokiol and Magnolol Using High-Capacity High-Speed Counter-current Chromatography. *J Chromatogr. A* **2007**, *1142*, 115–122.
25. Jeong, B.; Choi, Y. K.; Bae, Y. H.; Zentner, G.; Kim., S. W. New Biodegradable Polymers for Injectable Drug Delivery Systems. *J. Controlled Release* **1999**, *62*, 109–114.
26. Li, J.; Li, X.; Ni, X.; Leong, K. W. Synthesis and Characterization of New Biodegradable Amphiphilic Poly(ethylene oxide)-*b*-Poly[(*R*)-3-hydroxybutyrate]-*b*-Poly(ethylene oxide) Triblock Copolymers. *Macromolecules* **2003**, *36*, 2661–2667.
27. Xiong, X. Y.; Tam, K. C.; Gan, L. H. Synthesis and Aggregation Behavior of Pluronic F127/Poly(lactic acid) Block Copolymers in Aqueous Solutions. *Macromolecules* **2003**, *36*, 9979–9985.
28. Liu, C. B.; Gong, C. Y.; Huang, M. J.; Wang, J. W.; Pan, Y. F.; Zhang, Y. D.; Li, G. Z.; Gou, M. L.; Wang, K.; Tu, M. J.; Wei, Y. Q.; Qian, Z. Y. Thermoreversible Gel−Sol Behavior of Biodegradable PCL−PEG−PCL Triblock Copolymer in Aqueous Solutions. *J. Biomed. Mater. Res., Part B* **2008**, *84*, 165–175.
29. Zhou, S. B.; Deng, X. M.; Yang, H. Biodegradable Poly(ε-caprolactone)-poly(ethylene glycol) Block Copolymers: Characterization and Their Use as Drug Carriers for a Controlled Delivery System. *Biomaterials* **2003**, *24*, 3563–3570.
30. Li, J.; Ni, X.; Li, X.; Tan, N. K.; Lim, C. T.; Ramakrishna, S.; Leong, K. W. Micellization Phenomena of Biodegradable Amphiphilic Triblock Copolymers Consisting of Poly(ε-hydroxyalkanoic acid) and Poly(ethylene oxide). *Langmuir* **2005**, *21*, 8681–8685.
31. Li, J.; Li, X.; Ni, X.; Wang, X.; Li, H.; Leong., K. W. Self-Assembled Supramolecular Hydrogels Formed by Biodegradable PEO−PHB−PEO Triblock Copolymers and ε-Cyclodextrin for Controlled Drug Delivery. *Biomaterials* **2006**, *27*, 4132–4140.
32. Liu, C. B.; Gong, C. Y.; Pan, Y. F.; Zhang, Y. D.; Wang, J. W.; Huang, M. J.; Wang, Y. S.; Wang, K.; Gou, M. L.; Tu, M. J.; Wei, Y. Q.; Qian, Z. Y. Synthesis and Characterization of a Thermosensitive Hydrogel Based on Biodegradable Amphiphilic PCL-Pluronic(L35)-PCL block Copolymers. *Colloids Surf., A* **2007**, *302*, 430–438.
33. Gong, C. Y.; Wu, Q. J.; Bing, Kan; Zhao, X.; Dong, P. W.; Xie, Y.; Wei, Y. Q.; Qian, Z. Y. Acute Toxicity Evaluation of Biodegradable Thermosensitive Hydrogel Controlled Drug Delivery System Based on PEG−PCL−PEG Copolymer. *J. Biomed. Mater. Res. B* **2009**, *91B*, 26–36.
34. Ahn, K. S.; Sethi, G.; Shishodia, S.; Sung, B.; Arbiser, J. L.; Aggarwal, B. B. Honokiol Potentiates Apoptosis, Suppresses Osteoclastogenesis, and Inhibits Invasion through Modulation of Nuclear Factor-κB Activation Pathway. *Mol Cancer Res.* **2006**, *4*, 621–633.
35. Momi, H.; Matsuyama, W.; Inoue, K.; Kawabata, M.; Arimura, K.; Fukunaga, H.; Osame, M. Vascular Endothelial Growth Factor and Proinflammatory Cytokines in Pleural Effusions. *Respir. Med.* **2002**, *96*, 817–822.
36. Hamed, E. A.; El-Noweihi, A. M.; Mohamed, A. Z.; Mahmoud, A. Vasoactive Mediators (VEGF and TNF-α) in Patients with Malignant and Tuberculous Pleural Effusions. *Respirology* **2004**, *9*, 81–86.
37. Sack, U.; Hoffman, M.; Zhao, X. J.; Chan, K. S.; Hui, D. S.; Gosse, H; Engelmann, L.; Hoheisel, G.; Schauer, J.; Emmrich, F. Vascular Endothelial Growth Factor in Pleural Effusions of Different Origin. *Eur. Respir. J.* **2005**, *25*, 600–604.
38. Sheu, M. L.; Liu, S. H.; Lan, K. H. Honokiol Induces Calpain-Mediated Glucose-Regulated Protein-94 Cleavage and Apoptosis in Human Gastric Cancer Cells and Reduces Tumor Growth. *PLoS One* **2007**, *2*, e1096.
39. Wang, T.; Chen, F.; Chen, Z.; Wu, Y. F.; Xu, X. L.; Zheng, S.; Hu, X. Honokiol Induces Apoptosis through p53-Independent Pathway in Human Colorectal Cell Line RKO. *World J. Gastroenterol.* **2004**, *10*, 2205–2208.
40. Park, E. J.; Zhao, Y. Z.; Kim, Y. H.; Lee, B. H.; Sohn, D. H. Honokiol Induces Apoptosis *via* Cytochrome *c* Release and Caspase Activation in Activated Rat Hepatic Stellate Cells *in Vitro*. *Planta Med.* **2005**, *71*, 82–84.
41. Yuan, Z. P.; Chen, L. J.; Fan, L. Y.; Tang, M. H.; Yang, G. L.; Yang, H. S.; Du, X. B.; Wang, G. Q.; Yao, W. X.; Zhao, Q. M.; *et al*. Liposomal Quercetin Efficiently Suppresses Growth of Solid Tumors in Murine Models. *Clin. Cancer Res.* **2006**, *12*, 3193–3199.
42. Li, G.; Tian, L.; Hou, J. M.; Ding, Z. Y.; He, Q. M.; Feng, P.; Wen, Y. J.; Xiao, F.; Yao, B.; Zhang, R.; *et al*. Improved Therapeutic Effectiveness by Combining Recombinant CXC Chemokine Ligand 10 with Cisplatin in Solid Tumors. *Clin. Cancer Res.* **2005**, *11*, 4217–4224.